Eur. Phys. J. AP **20**, 141–144 (2002)
DOI: 10.1051/epjap:2002084

THE EUROPEAN PHYSICAL JOURNAL APPLIED PHYSICS

Development of an UV scanning photoluminescence apparatus for SiC characterization*

L. Masarotto, J.M. Bluet[a], M. Berenguer, P. Girard, and G. Guillot

Laboratoire de Physique de la Matière[b], Institut National des Sciences Appliquées de Lyon, 7 avenue Jean Capelle, 69621 Villeurbanne Cedex, France

Received: 21 November 2001 / Received in final form: 18 June 2002 / Accepted: 20 June 2002
Published online: 25 October 2002 –

Abstract. We have adapted a scanning photoluminescence (SPL) apparatus, previously developed for III-V compounds analysis, for the characterization of SiC. The PL mapping is obtained by scanning the sample, fixed to an x-y stage with 1 μm minimal step, under a doubled Ar^+ laser beam (244 nm) focused by a microscope objective (×52). For this excitation the spot diameter is about 4 μm. The PL signal can be either directly detected, giving integrated PL intensity, either dispersed using a monochromator, giving spectrally resolved PL (1 nm resolution). The measurements can be realized at room temperature for near band edge studies, or at low temperature (80 K) for deep defects investigation. The gettering effect of non radiative centres by the screw dislocations in 6H-SiC is evidenced using this apparatus.

PACS. 78.55.Ap Elemental semiconductors

1 Introduction

There are nowadays both a strong research activity and industrial developments toward the future marketing of high power devices realized on silicon carbide (SiC). Indeed, SiC is recognized as the most adapted semiconductor for the realization of electronic devices working in harsh conditions. Its large band gap (3.2 eV for the 4H polytype), its high electron drift velocity (2×10^7 cm s^{-1}), its high breakdown field (2.5×10^6 V cm^{-1}), and its high thermal conductivity (4.9 W cm^{-1}) are particularly interesting for high temperature, high power and high frequency applications. Moreover, there are now several commercial source of SiC wafers.

During the last several years, tremendous progress in SiC bulk growth and epitaxy has been realised. Nevertheless, the material quality is still poor in comparison with the other semiconductors which are used in the microelectronic industry (Si, GaAs). Indeed, the non uniformity of impurity and crystalline defect (dislocation, micropipes, grain boundaries...) distribution in SiC wafers (particularly in semi-insulating one) and the doping inhomogeneities of the epitaxial layers still act as show-stopper for high performance and high reliability devices development. This is why a spatially resolved, non destructive and few time consuming characterization tool is strongly needed for a tight quality control of the wafers.

The photoluminescence of SiC has been widely studied since the 60s. Many works have dealt with the different radiative recombination process: free exciton recombination, donors (N, P) and acceptors (Al, Ga) bound exciton recombination, donor acceptor pair recombination and numerous recombination due to the presence of deep levels. Intra-band recombination of transition metal has also been observed [1]. An exhaustive review of these works has been published by Devaty and Choyke [2].

The measurement of the SiC photoluminescence is then usefull for the study of the electrical properties (free carriers lifetime, doping level), of strain and of defects. The interest of scanning photoluminescence is then, obviously, to get informations about the lateral uniformity of these properties. For instance, the method has been successfully utilized for the characterization of the dominant midgap donor EL2 in semi-insulating GaAs wafers [3], for dislocations mapping in InP and GaAs bulks and epitaxial layers [4–6], and for revealing oxygen precipitates [7,8] and dislocations [9] in Si wafers. The first results related to SiC [10,11] indicates that PL imaging is a very promising tool for material characterization. This is why we have adapted an integrated PL imaging system from "SCANTEK" company in order to make integrated and spectrally resolved PL scanning for evaluation of SiC epitaxial layers and bulk wafers.

2 Experimental setup

Many modifications of the initial SCANTEK system has been realized in order to perform spectrally resolved measurement and for the adaptation for SiC characterization. The schematic principle of the measurement system is shown in Figure 1.

* This paper has been first presented orally at the C2I colloquium in February 2001

[a] e-mail: `bluet@insa.insa-lyon.fr`

[b] UMR 5511 CNRS

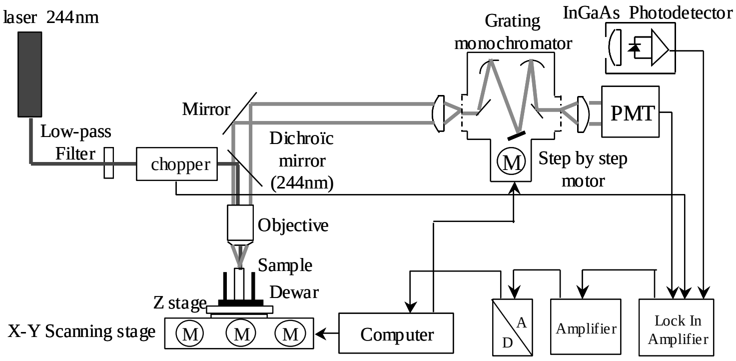

Fig. 1. Block diagram of the experimental setup.

Because of the SiC wide band gap, an UV excitation is necessary for the generation of carriers. Moreover, an important excitation density is necessary because of the low luminescence yield of SiC which has an indirect band gap. The conventional optic components have been replaced by specific UV ones in order to prevent parasitic fluorescence and to optimize both the excitation and the collection efficiency. A monochromator, controlled by the computer, has been added to the original system in order to perform spectrally resolved PL mappings. Finally, in order to optimize the PL signal and to measure recombination inaccessible at room temperature (donor -acceptor pair recombination for instance) a simple cryogenic system has been conceived. Schematically, it consists in a metal cylinder steeping in liquid nitrogen inside an open dewar. The principal technical characteristics of the system with a focus on the optics of excitation and collection are described in the following.

In Figures 2 and 3 are described the different optical components used for the excitation and the collection. The frequency doubled argon laser beam (244 nm) is modulated by a chopper. The chopper frequency is the reference frequency for the Lock-in amplifier. We have chosen in order to optimize the signal to noise ratio to average over ten periods and to fix the undulation rate at 5%. This assign the frequency as a function of the lock-in time constant. A wavelength low pass filter (cut-off frequency: 400 nm) has been added in order to cut parasitic wavelength (at 488 nm for instance). The beam is then directed toward the objective by a dichroïc mirror which reflects 99% of the incident beam at 244 nm. Finally the beam is focused by an achromatic mirror objective with a magnification of 52 and a focal length of 3.6 mm (f_1). The total incident power on the sample is of 10% of the initial laser one. The measured laser spot diameter on the sample is of 3 μm which gives to the apparatus a very good spatial resolution. Nevertheless, the spatial resolution in most cases is given by the excited carrier diffusion length which, for SiC, is ranging between few micrometers up to 40 μm depending on the crystal quality and purity. The photoluminescence signal is then collected by the same objective which, owing to its important numerical aperture (0.7), gives a good collection ratio. The reflection from the sample and fluorescence coming from optical component are then filtered by two wavelength high-pass filter (cut-off frequency of 235 nm and 280 nm). The PL signal is then directed toward the monochromator and focused by a silica lens of 50 mm focal length (f_2) (BENTHAM TM 300). This focal length has been chosen in order to obtain a beam width at entrance slit (w) inferior to 100 μm ($w = f_1/f_2 \times$ surface of emission). The monochromator turret, controlled from the computer, holds a mirror for integrated PL intensity measurements and two gratings for spectral measurements in the 0.3–1.8 μm spectral range. The spectral resolution is 1 nm. The total collection factor defined as the ratio between the PL intensity inside the semiconductor and the PL intensity received by the photomultiplier is of 8×10^{-4}.

In the UV-visible range the PL is detected by a photomultiplier with a GaAs photocathode (HAMAMATSU 5701). The electric signal is then amplified by the lock-in amplifier (EG&G 5209). The software analyzes the PL spectrum and gives mapping of the main peak parameters (wavelength at maximum, intensity and width at half maximum). The mapping is provided by an x-y stage with a maximum course of 102 mm and a minimal step of 1 μm.

3 Results and discussion

The samples used in the present study are n-type (10^{16} cm^{-3}) 6H SiC epitaxial layers purchased from a commercial source. First, integrated PL images have been realized. On all the investigated samples, an arbitrary distribution of bright spots (high PL intensity) has been observed. Their density is ranging between 6×10^3 cm^{-2} and 1.2×10^4 cm^{-2} depending on the sample. On the samples periphery well defined lines formed by closely spaced bright spots were also observed. An example showing 20 of these high PL intensity cells is displayed in Figure 4. Their dimension is ranging between few micrometers to 20 μm. For the three whiter ones, an asymmetric intensity pattern with extension of the bright zone along a preferential direction is clearly observed. For the brightest zones the integrated PL intensity is approximately one order of magnitude higher than in the rest of the sample. The density of these bright spots and their distribution imply that they are due to elementary screw dislocations. In order to confirm this hypothesis and to analyse the origin of this localized PL intensity exhausts we have next performed

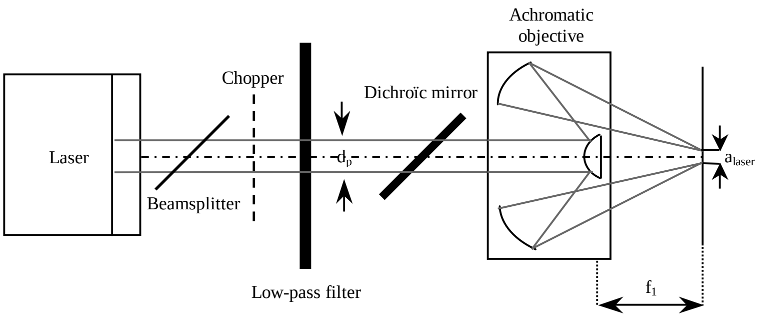

Fig. 2. Excitation optical path.

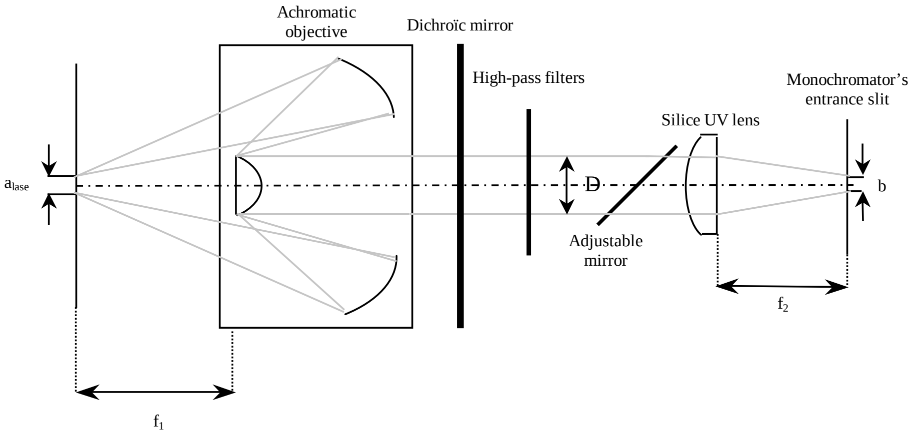

Fig. 3. Collection optical path.

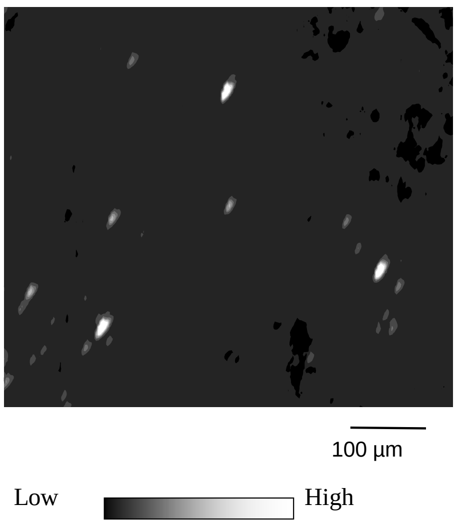

Fig. 4. Integrated PL intensity mapping of a 0.6×0.6 mm^2 area of a 6H-SiC epitaxy.

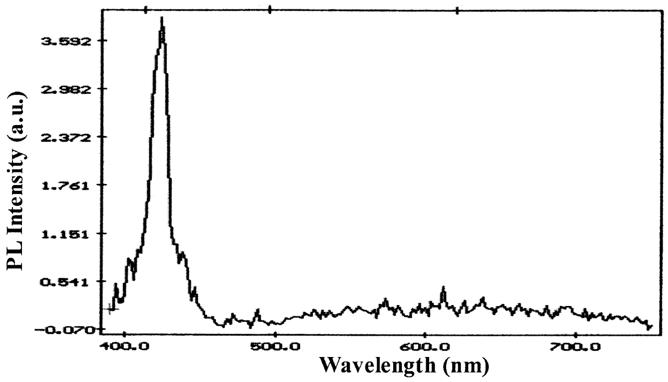

Fig. 5. Typical room temperature spectrum for a 6H-SiC epitaxy.

spectral PL mapping in the range 400–800 nm with high spatial resolution. Either on the high intensity regions or around them, only near band edge PL signal was found. It consists of a predominant peak at 420 nm and a shoulder on the lower energy side at 435 nm (Fig. 5). This correspond to previously reported values obtained in classical PL measurement [12]. High spatial resolution mapping of the spectral parameters for the predominant near band edge peak are displayed in Figure 6. Figure 6a is an integrated PL mapping realized around a bright spot described above. Figures 6b and 6c are respectively the intensity mapping and the full width at half maximum (FWHM) mapping of the 420 nm peak in the same spatial zone.

We clearly obtain a very good correlation between the integrated PL scanning image and the spectral parameters ones. Classical PL measurement as a function of temperature revealed that N bound exciton lines disappear above 100 K in our samples. In consequence, the peak at 2.98 eV measured at room temperature arises from band to band

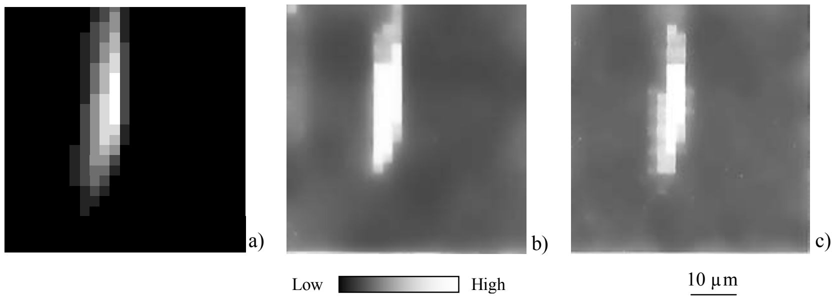

Fig. 6. Pl mapping of a bright zone with a 3 μm spatial resolution. (a) Integrated PL intensity, (b) 2.98 eV near band edge peak intensity, (c) full width at half maximum for this peak.

recombination. In this case, the luminescence intensity is limited by the recombination *via* non radiative traps acting as lifetime killer centres. Furthermore, no additional line due to impurity is observed either away from a bright or in a bright spot. Therefore we attribute the local enhancement of the PL to a cleaning of lifetime killer centres in these zones. This phenomenon has been observed in liquid encapsulated Czochralski (LEC) GaAs and attributed to the presence of dislocations [13]. Indeed, impurities and microdefects can be gettered by the strain field existing in the neighbourhood of an extended defect like a dislocation. These results in a local cleaning of a zone around the defect much greater than the defect itself which is known as the denuded zone. In our case, we think that the bright spots we observe, are due to denuded zones in the vicinity of elementary screw dislocations. In this hypothesis, we should observe a small dark point in the centre of the bright cell corresponding to the decorated dislocation core which was not found even with 1 μm spatial resolution. This can be due either to an insufficient spatial resolution or to the lateral diffusion length of the exciton greater than the spatial resolution. The FWHM observed in Figure 3c is relatively important with a relative variation of 20%. This peak width enhancement is also consistent with the presence of a dislocation. Indeed, the strain field in the dislocation boundary implies modifications of the band structure resulting in the enlargement of the peak. This phenomenon has been clearly observed for InP and Si doped GaAs [4].

From the previous discussion we so propose that the bright spots observed in our integrated measurements are due the denuded zone around screw dislocations. Nevertheless we cannot conclude that all the integrated PL intensity come from the near band edge recombination. Indeed some infrared contribution due to gettered metallic impurity like V can also be included in the integrated PL signal. The spectral extension of our equipment in this region, described in Section 2, will give us information on this possible effect.

4 Conclusion

A unique PL scanning apparatus, working in the UV range (244 nm for excitation), has been developed with a spatial resolution of 1 μm, a scanned area up to 10 $\times$ 10 cm^2, a spectral resolution of 1 nm and a spectral range cover from 0.3 μm to 1.7 μm. Using this equipment, we have evidenced the gettering effect, due to the strain field, of microdefects acting as lifetime killer centres around the elementary screw dislocations in 6H-SiC epitaxial layers. The understanding of this gettering effect is of crucial importance for the development of SiC devices. For instance, the presence of minority carrier lifetime killers in the screw dislocations vicinity is detrimental for bipolar devices applications. Recently, we found the same results for 4H-SiC substrates.

Financial support was received from the Rhône-Alpes region.

References

1. V. Seguier, Études electro-optiques de matériaux SiC : Contribution à l'analyse de l'impureté Vanadium, Thèse de doctorat, INSA de Lyon, 1999
2. R.P. Devaty, W.J. Choyke, Phys. Stat. Sol. A **162**, 5 (1997)
3. M. Tajima, Appl. Phys. Lett. **53**, 959 (1988)
4. C. Klingelhoffer, Ph.D. Thesis, École Centrale de Lyon, 1995
5. M.K. Nuban, Ph.D. Thesis, École Centrale de Lyon, 1996
6. P. Bunod, Ph.D. Thesis, University Joseph Fourier of Grenoble, 1989
7. M. Tajima, T. Masui, T. Abe, *Semiconductor Silicon 1990*, edited by H.R. Huff, K.G. Barraclough, J. Chiwaka (Electrochem. Soc., Pennington, 1990), p. 994
8. Y. Kitagawara, R. Hoshi, T. Takenaka, J. Electrochem. Soc. **139**, 2277 (1992)
9. J.L. Weyher, P.J. Van der Wel, C. Frigeri, Semicond. Sci. Technol. **7**, A294 (1992)
10. M. Tajima, Y. Kumagaya, T. Nakata, M. Inoue, A. Nakamura, Mater. Sci. Forum **264-268**, 481 (1998)
11. M. Tajima, Y. Kumagaya, T. Nakata, M. Inoue, A. Nakamura, Jpn. J. Appl. Phys. **36**, L1185 (1998)
12. A. Henry, J.P. Bergman, O. Kordina, C. Hallin, I.G. Ivanov, E. Janzen, Inst. Phys. Conf. Ser. **142**, 357 (1996)
13. S.K. Krawczyk, *Encyclopaedia of Advanced Materials* (Pergamon Press Oxford, 1994), p. 2318